JCTC Journal of Chemical Theory and Computation

Article

Cite This: J. Chem. Theory Comput. 2018, 14, 1198−1205

pubs.acs.org/JCTC

# Floquet Study of Quantum Control of the Cis−Trans Photoisomerization of Rhodopsin

Pablo E. Videla,[†,‡] Andreas Markmann,[†,‡] and Victor S. Batista*[,†,‡]

[†]Department of Chemistry, Yale University, P.O. Box 208107, New Haven, Connecticut 06520-8107, United States

[‡]Energy Sciences Institute, Yale University, P.O. Box 27394, West Haven, Connecticut 06516-7394, United States

**ABSTRACT:** Understanding how to control reaction dynamics of polyatomic systems by using ultrafast laser technology is a fundamental challenge of great technological interest. Here, we report a Floquet theoretical study of the effect of light-induced potentials on the ultrafast cis−trans photoisomerization dynamics of rhodopsin. The Floquet Hamiltonian involves an empirical 3-state 25-mode model with frequencies and excited-state gradients parametrized to reproduce the rhodopsin electronic vertical excitation energy, the resonance Raman spectrum, and the photoisomerization time and efficiency as probed by ultrafast spectroscopy. We simulate the excited state relaxation dynamics using the time-dependent self-consistent field method, as described by a 3-state 2-mode nuclear wavepacket coupled to a Gaussian ansatz of 23 vibronic modes. We analyze the reaction time and product yield obtained with pulses of various widths and intensity profiles, defining 'dressed states' where the perturbational effect of the pulses is naturally decoupled along the different reaction channels. We find pulses that delay the excited-state photoisomerization for hundreds of femtoseconds, and we gain insights on the underlying control mechanisms. The reported findings provide understanding of quantum control, particularly valuable for the development of ultrafast optical switches based on visual pigments.

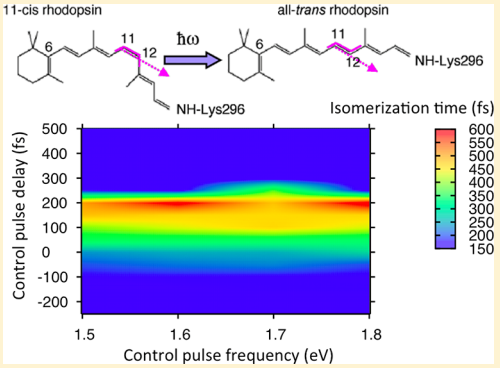




## 1. INTRODUCTION

Understanding the effect of strong electromagnetic fields on the relaxation dynamics of molecules is a problem of great fundamental and technological interest. A wide range of laser techniques, including methods with femtosecond and attosecond time resolution, has already been developed to probe and control a variety of molecular processes.[1−9] Here, we implement Floquet theory to study the influence of femtosecond laser pulses on the ultrafast reaction dynamics of isomerization of visual rhodopsin upon photoexcitation to the $S_1$ electronic excited state.[10−17]

Floquet theory has been applied to analyze quantum dynamics of diatomic molecules as influenced by strong electric fields.[18−21] Earlier studies have shown that strong laser fields induce molecular alignment in optical lattices by coupling vibrational and rotational degrees of freedom.[22] In addition, strong running or standing laser waves give rise to a variety of nonadiabatic phenomena that couple translational and internal rovibronic motions and reduce the efficiency of molecular trapping in optical lattices.[23,24] The use of moderately strong resonant pulses (e.g., with intensity of tens of TW/cm$^2$) has been shown to modulate bond softening/hardening by changing the bond length of diatomics.[25−27] However, the relaxation dynamics of more complex systems such as the retinyl chromophore of rhodopsin undergoing cis−trans isomerization has yet to be explored with Floquet theory.

Floquet theory describes light-molecule interactions in terms of "dressed states" (i.e., molecular states that are shifted in energy according to the perturbational field frequency and intensity). The dressed states determine effective Light-Induced Potentials (LIP) with the usual topological features of multidimensional potential energy surfaces (PES) such as avoiding crossings and conical intersections (CI).[24,27] In particular, Light-Induced Conical Intersections (LICI) due to nonadiabatic couplings break down the Born−Oppenheimer adiabatic approximation and induce nonadiabatic transitions. The resulting LIP can dramatically influence the photoinduced reaction dynamics and can thus be tailored to control the reaction times and mechanisms in excited states.[22,23,25,26,28−35]

LIP and LICI generated by strong pulses have been shown to modulate the nuclear quantum dynamics of small polyatomic systems.[36−38] For example, a LICI has been exploited to influence the dissociation rate and vibrational population of the NO fragment of *cis*-methyl nitrite as a function of the polarization state of the incident beam.[36] Fields that generate LIP and LICI in the PES of $CH_3I$ have been shown to influence the yield of photodissociation dynamics and the velocities of the photoproduct fragments.[37] In addition, LICI have been used to understand the yield of pothoisomerization of 1,3-cyclohexadiene under the influence of strong fields.[38] Here, we

Received: December 3, 2017
Published: February 9, 2018




DOI: 10.1021/acs.jctc.7b01217
J. Chem. Theory Comput. 2018, 14, 1198−1205

investigate the cis−trans isomerization of the retinyl chromophore in rhodopsin as influenced by moderately strong laser pulses that generate LIP. The reaction is an ultrafast photoisomerization that generates the trans retinyl isomer within 200 fs after photoexcitation of the dark adapted retinyl pigment in the cis form. Understanding to what extent quantum control of rhodopsin can be achieved remains a fundamental problem of great interest in physical chemistry as well as for the development of ultrafast molecular optical switches.

Previous studies have shown that a modest level of quantum control can be achieved in rhodopsin by using pulse-shaping techniques designed to maximize/minimize the population of the trans ground state,[10−12] including the implementation of a bichirped coherent control scenario based on tuning of relative phases of two overlapping photoexcitation pulses.[11] However, it remains to be established whether more extensive control can actually be achieved by rational design of ultrafast pulses or even in terms of incoherent control as recently proposed.[15,16]

Here, we focus on the effect of the LIP generated by moderately strong laser pulses, as simulated by the Floquet formalism.[18−21] The isomerization dynamics is described by an empirical model Hamiltonian,[39,40] implemented in earlier studies,[11,13] parametrized to reproduce the rhodopsin electronic vertical excitation energy, the resonance Raman spectroscopy,[41] and the photoisomerization time and efficiency as probed by ultrafast spectroscopy.[42] Since our objective is to understand the effect of strong fields on the cis−trans isomerization process, we explore a simple and hence experimentally feasible pulse scheme. Our results provide valuable insights into branching processes and demonstrate the feasibility of using LIP to manipulate the underlying photoisomerization as necessary for ultrafast optical switches based on quantum control of the cis/trans interconversion.

The paper is organized as follows. Section 2 describes the model system and computational approach implemented for the description of quantum dynamics. Section 3 presents the results and a discussion of the effect of laser pulses on the dynamics of photoisomerization. Section 4 summarizes and concludes.

## 2. METHODS

**2.1. Model Hamiltonian.** Previous studies have shown that the cis−trans photoisomerization of rhodopsin can be modeled by the time-independent 2-state 25-mode model Hamiltonian, $\hat{H}_0 = \hat{H}_M(\theta,x) + \hat{H}_B(\mathbf{z})$.[11,13,39,40] The model explicitly accounts for the collective torsional coordinate $\theta$ and delocalized stretching vibrational mode of the polyene chain $x$, as well as the "bath" of Condon-active vibrational modes $\mathbf{z} = \{z_i\}$. The functional form of the Hamiltonian is[39]

$$\hat{H}_M(\theta, x) = \sum_{n=0}^{1}\sum_{m=0}^{1} |n\rangle H_{nm}\langle m| \tag{1}$$

$$\hat{H}_B(\mathbf{z}) = \sum_{n=0}^{1} |n\rangle\langle n| \sum_{i=1}^{23} \frac{\omega_i}{2}(z_i^2 + p_i^2) + (1-\delta_{0n})c_i z_i \tag{2}$$

where $|0\rangle$ and $|1\rangle$ are the diabatic ground and excited electronic states, respectively, with

$$H_{00} = T + V_0 \tag{3}$$

$$H_{11} = T + V_1 \tag{4}$$

$$H_{01} = H_{10} = \lambda_x x \tag{5}$$

$$T = -\frac{1}{2m}\frac{\partial^2}{\partial\theta^2} - \frac{\omega_x}{2}\frac{\partial^2}{\partial x^2} \tag{6}$$

$$V_0 = \frac{W_1}{2}(1-\cos(\theta)) + \frac{\omega_x}{2}x^2 \tag{7}$$

$$V_1 = E_2 - \frac{W_2}{2}(1-\cos(\theta)) + \frac{\omega_x}{2}x^2 + k_x x \tag{8}$$

The parameters of the model Hamiltonian,[39] introduced by eqs 1 and 2, are defined to reproduce the electronic vertical excitation energy, energy storage, and the resonance Raman spectroscopy spectrum of rhodopsin,[41] as well as the photoisomerization time and efficiency as probed by ultrafast spectroscopy.[42] More realistic models of the cis−trans isomerization of rhodopsin, based for example on quantum-mechanics/molecular-mechanics (QM/MM) hybrid methods,[43−46] would be desired but have yet to be developed. Nevertheless, the semiempirical model Hamiltonian implemented in our studies allows for the investigation of essential features of the light-induced photoisomerization and is an ideal starting point to analyze the effect of LIP on nonadiabatic dynamics within the Floquet formalism.

In the presence of the laser field, the dynamics of the system is ruled by the time-dependent Hamiltonian

$$\hat{H}(t) = \hat{H}_0 + \hat{V}(t) \tag{9}$$

where $\hat{V}(t)$ defines the interaction of the system with the control laser field under the dipole approximation

$$\hat{V}(t) = |0\rangle\langle 1|g(t)\cos(\omega t)\mu\cdot\varepsilon_0 + cc \tag{10}$$

Here, $\mu$ is the dipole moment of the system (taken, hereafter, as 1 au), $\varepsilon_0$ and $\omega$ are the peak amplitude and frequency of the control pulse, and $g(t)$ is the pulse envelope, modeled as a $\cos^2$ profile of the form

$$g(t) = \begin{cases} \cos^2\left(\pi\dfrac{(t-t_p)}{t_d}\right), & \text{if } |t-t_p| < t_d/2 \\ 0, & \text{otherwise} \end{cases} \tag{11}$$

where $t_p$ is the pulse center (i.e., the time at which the pulse reaches its maximum intensity) and $t_d$ is the time duration of the pulse.

**2.2. Floquet Representation.** The Hamiltonian introduced by eq 9 can be used to analyze the quantum dynamics of the system as influenced by perturbational pulses, according to the Floquet representation of quantum mechanics[18−21] which often provides valuable insights in terms of the effect of LIP. In the Floquet picture, it is useful to define composite basis states $|n,\alpha\rangle$ defined as the product of physical states $|n\rangle$ and the Fourier space basis $|\alpha\rangle$ with $\langle t|\alpha\rangle = e^{i\alpha\omega t}$ ($\alpha$ integer) and period $T = 2\pi/\omega$. Extending the basis of the time-dependent Hamiltonian introduced by eq 9 accordingly, we obtain the so-called 'Floquet Hamiltonian' with matrix elements defined, as follows:

$$\langle n,\alpha|\hat{H}_F(t)|m,\beta\rangle = \frac{1}{T}\int_0^T dt e^{i(\beta-\alpha)\omega t}\langle n|\hat{H}(t)|m\rangle \tag{12}$$

Assuming that the pulse is much longer than the field period, the matrix elements introduced by eq 12 can be simplified, as follows[30,47,48]



DOI: 10.1021/acs.jctc.7b01217
J. Chem. Theory Comput. 2018, 14, 1198−1205

$$\langle n, \alpha|\hat{H}_F(t)|m, \beta\rangle = (\langle n|\hat{H}_0|m\rangle + \alpha\omega\delta_{n,m})\delta_{\alpha,\beta} + F_{01}(t)(1 - \delta_{n,m})\delta_{\alpha,\beta=\alpha\pm1} \quad (13)$$

where

$$F_{01}(t) = F_{10}(t) = \frac{1}{2}\mu\cdot\varepsilon_0 g(t) \quad (14)$$

According to eq 13, the Floquet Hamiltonian consists of an infinite dimensional matrix with diagonal elements defined by 'dressed' states (i.e., physical states shifted in energy according to the field frequency) and nondiagonal terms that couple only adjacent Fourier states (i.e., states with $|\beta\rangle = |\alpha \pm 1\rangle$). When the pulse envelope $g(t)$ is approximately constant, the Floquet Hamiltonian becomes time-independent, and the Floquet theory of periodic Hamiltonians is recovered.

Formally, the Floquet Hamiltonan introduced by eq 13 is of infinite dimension. However, only a few Floquet channels $\alpha$ are actually coupled during the finite-time dynamics, as defined by the time-dependence of nondiagonal elements. Floquet states that are never populated while the pulse is active can be safety neglected in the Hamiltonian (13) without affecting the dynamical evolution of the system. Considering that the cis−trans isomerization is an ultrafast process, we find that the dynamics can be accurately described according to a 3-state Hamiltonian, defined by the basis of ground and excited electronic states $|0,0\rangle \equiv |0\rangle$ and $|1,0\rangle \equiv |1\rangle$, respectively, and the Floquet shifted channel defined by the ground dressed state $|0,1\rangle \equiv |0+\omega\rangle$, as follows:

$$H_F(t) = \begin{pmatrix} H_{00} & H_{01} & 0 \\ H_{10} & H_{11} & F_{01}(t) \\ 0 & F_{10}(t) & H_{00} + \hbar\omega \end{pmatrix} \quad (15)$$

An advantage of using the Floquet Hamiltonian introduced by eq 15, over simulations simply based on the Hamiltonian introduced by eq 9, is that LIP and LICI arise naturally in the Floquet representation and allow for simple interpretations of the effect of the field on the underlying relaxation dynamics.

Figure 1 shows the diabatic PES corresponding to the Floquet Hamiltonian for $x = 0$, along the dihedral angle $\theta$. The surfaces include the ground and excited state potentials $V_0$ and $V_1$, respectively, as well as the dressed Floquet state, $V_0 + \hbar\omega$.

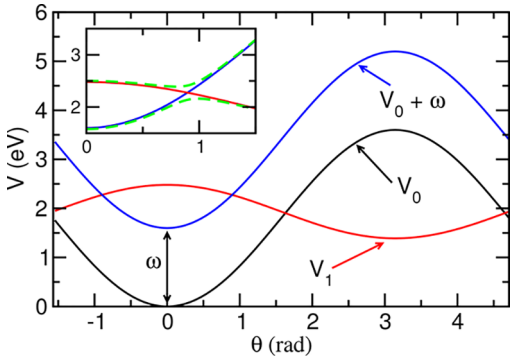


**Figure 1.** Diabatic PES cuts along the dihedral angle $\theta$ for $x = 0$ for the Floquet Hamiltonian eq 15, corresponding to a control pulse with $\hbar\omega$ = 1.6 eV. Inset: close-up of the region near $\theta_{LIP}$. Green dashed lines correspond to the resulting adiabatic potentials for a field intensity of $\varepsilon_0$ = 0.01 au.

We note that the curve-crossing between dressed and excited states, at $\theta = \theta_{LIP}$ along the isomerization coordinate, depends on the frequency of the control field. Increasing or decreasing the frequency of the field brings the position of $\theta_{LIP}$ closer to the Franck−Condon or Conical Intersection regions, respectively. Hence, the role of the frequency under the Floquet representation is to determine the position of the LIP/LICI on the PES. Figure 1 (inset) shows the resulting LIP obtained for a field intensity of $\varepsilon_0$ = 0.01 au. As shown below, the LIP greatly influences the dynamics of isomerization and depends on the coupling $F_{01}(t)$ and, hence, on the parameters of the field.

**2.3. Physical Observables.** The electronic space including states $|0\rangle$ and $|1\rangle$ is extended in the Floquet representation with the dressed state $|0 + \hbar\omega\rangle$. So, it is necessary to describe how to compute physical observables in such an extended representation. For the case of the Hamiltonian introduced by eq 15, the time-dependent nuclear wavepacket involves three components, as follows

$$\chi(\mathbf{x}; t) = \chi_0(\mathbf{x}; t)|0\rangle + \chi_1(\mathbf{x}; t)|1\rangle + \chi_{0+\hbar\omega}(\mathbf{x}; t)|0 + \hbar\omega\rangle \quad (16)$$

where $\mathbf{x} = (\theta,x)$ and $\chi_j(\mathbf{x};t)$ represent the nuclear wavepacket component of the Floquet diabatic state $|j\rangle$. At this point, it is useful to recall that for any Floquet state $|j\rangle$ with quasienergy $E_j$, multiplication by a phase factor $e^{in\omega t}$ (with $n$ integer) yields another Floquet state with quasienergy $E_j + n\hbar\omega$.[18−21] Therefore, the physically meaningful diabatic nuclear wave functions can be expressed as a sum over all shifted Floquet states, as follows[48]

$$\chi_{[\alpha]}(\mathbf{x}; t) = \sum_n e^{in\omega t}\chi_{\alpha+n\hbar\omega}(\mathbf{x}; t) \quad (17)$$

where $\alpha = (0,1)$ represents the electronic state. Taking the square modulus and neglecting the fast oscillatory term (or equivalently, making an average over one pulse cycle $T$) the diabatic population can be expressed, as follows:

$$\rho_{[\alpha]}(\mathbf{x}; t) = \sum_n |\chi_{\alpha+n\hbar\omega}(\mathbf{x}; t)|^2 \quad (18)$$

From eq 17, the nuclear wave function in the adiabatic ground $(S_0)$ and excited $(S_1)$ states can be computed, as follows

$$\chi^\beta(\mathbf{x}; t) = U_0^\beta(\mathbf{x})\cdot\chi_{[0]}(\mathbf{x}; t) + U_1^\beta(\mathbf{x})\cdot\chi_{[1]}(\mathbf{x}; t) \quad (19)$$

where $\beta = (S_0,S_1)$ and $U_\alpha^\beta$ are the elements of the eigenvectors of the matrix defined in the $|0\rangle,|1\rangle$ subspace. Taking the square modulus and averaging over a pulse cycle, the population of the adiabatic ground $(S_0)$ and excited $(S_1)$ states is obtained, as follows:

$$\tilde{\rho}^\beta(\mathbf{x}; t) = |U_0^\beta(\mathbf{x})|^2\cdot\rho_{[0]}(\mathbf{x}; t) + |U_1^\beta(\mathbf{x})|^2\cdot\rho_{[1]}(\mathbf{x}; t) \quad (20)$$

From the diabatic and adiabatic populations defined by eqs 18 and 20, respectively, it is possible to compute other properties of the system. For example, the cis adiabatic population is obtained, as follows

$$P_{cis}^\beta(t) = \int d\mathbf{x} h(\theta)\tilde{\rho}^\beta(\mathbf{x}; t) \quad (21)$$

where $h(\theta) = 1$, when $|\theta| < \pi/2$, and 0, otherwise. The trans adiabatic population is defined analogously by using the complementary function $[1 - h(\theta)]$.

**2.4. Computational Details.** The wavepacket propagation based on the Hamiltonian defined by eq 15 is performed


DOI: 10.1021/acs.jctc.7b01217
J. Chem. Theory Comput. 2018, 14, 1198−1205

according to the Split Operator Fourier Transform (SOFT) methodology,[49−51] in conjunction with the time-dependent self-consistent field (TDSCF) approximation.[11,52] According to the TDSCF approach,[11] the wavepacket is approximated by a single configurational Hartree ansatz

$$\psi(\mathbf{x}, \mathbf{z}; t) = e^{i\eta(t)}\phi(\mathbf{z}; t)\chi(\mathbf{x}; t) \tag{22}$$

where $\eta(t)$ is an overall phase and

$$\chi(\mathbf{x}; t) = \sum_j \chi_j(\mathbf{x}; t)|j\rangle \tag{23}$$

$$\phi(\mathbf{z}; t) = e^{\frac{i}{\hbar}S(t)} \prod_{k=1}^{23} \pi^{-1/4} e^{-(z_k - z_k(t))^2 + \frac{i}{\hbar}p_k(t)(z_k - z_k(t))} \tag{24}$$

with $S(t)$ representing the classical action for the classical trajectory of coordinates and momenta, $z_k(t)$ and $p_k(t)$, propagated by integration of Hamilton's equations, $\dot{z}_k = p_k$, and $\dot{p}_k = F_k$, using the mean-field effective forces, $F_k = -\sum_j \langle\chi_j|\partial H(t)/\partial z_k|\chi_j\rangle$. A swarm of initial conditions for the bath coordinates and momenta, $z_k(0)$ and $p_k(0)$, was sampled according to the ground vibrational states and evolved by using the Velocity-Verlet algorithm,[53] along with the time-dependent wavepacket components $\chi_j(\theta,x;t)$ which were represented on a regular grid of $2^8$ points for both $\theta$ and $x$ in the range of $|\theta| < \pi$ rad and $|x| < 5$ au. An integration time step of 10 au was used for all calculations.

We analyzed the dynamics of photoisomerization after instantaneously populating the excited electronic state $|1\rangle$ in the cis configuration by impulsive instantaneous excitation. The control pulse frequency was chosen to be $\hbar\omega = 1.6$ eV (≈775 nm) which gives a LIP at $\theta_{LIP} \approx 0.9$ rad, in between the Franck−Condon and the natural CI regions. To study the influence of the control pulse on the dynamics, we varied the pulse center $t_p$ from −150 to 320 fs in steps of 10 fs. Unless otherwise indicated, the peak amplitude $\varepsilon_0$ and pulse duration $t_d$ in eq 11 were set to 0.01 au ($I_0 \approx 3.5$ TW/cm$^2$) and 300 fs, respectively.

## 3. RESULTS AND DISCUSSION

We first analyze the dynamics of cis/trans isomerization in the absence of the control field−i.e., with $\varepsilon_0 = 0$ in eq 14. Under those conditions, the ground dressed state $|0+\omega\rangle$ is not coupled to the excited electronic state $|1\rangle$ since according to eq 15 the nondiagonal term $F_{01}$ is equal to zero. Hence, the system evolves freely after an impulsive excitation. Figure 2 shows the evolution of the time-dependent population of the retinyl in the cis $S_1$ adiabatic state ($P_{cis}^{S_1}$) and in the trans $S_0$ state ($P_{trans}^{S_0}$), consistent with simulations simply based on the Hamiltonian introduced by eq 9 without invoking Floquet theory.[11,13,40] The wave packet is initialized in the excited potential energy surface where it evolves following the gradient of the PES toward the natural conical intersection, located at $\theta \approx \pi/2$. After ∼100 fs, the wave packet reaches the CI and bifurcates, and some population transfers to the trans $S_0$ state. The population of the trans $S_0$ state continues to grow and reaches a maximum at $t \approx$ 180 fs. At subsequent times, part of the wave packet returns to the cis ground state, while the excited state component exhibits recurrences between cis and trans conformations and partitions with the ground state.[11,13,40] The observed recurrence is consistent with pump−probe experiments[42] and is due to partial decay of the photoproduct into the vibrationally hot cis ground state.[40] The observed dynamics in the absence of the control field is in agreement with previous simulations and shows that the model potential properly describes the isomerization reaction time and efficiency. We remark that the inclusion of dissipation due to coupling with a bath is expected to act on longer time-scales (>1 ps) and hence do not affect the results presented for the short-time process studied in this article.[54,55]

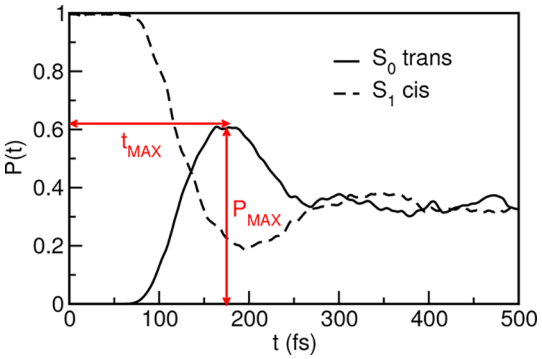


**Figure 2.** Time-dependent population dynamics in the absent of a control pulse. Highlighted in the figure are the parameters used to characterize the dynamics ($t_{MAX}$ and $P_{MAX}$).

For further analysis, we characterize the dynamics of the cis−trans isomerization in terms of two parameters, including $t_{MAX}$ and $P_{MAX}$, shown in Figure 2. The parameter $t_{MAX}$ is a measure of the isomerization time and describes the time at which the population of the trans $S_0$ state reaches the first maximum. The parameter $P_{MAX}$ is a measure of the isomerization efficiency and corresponds to the trans population at time $t_{MAX}$. As a reference, $t_{MAX} \approx 180$ fs and $P_{MAX} \approx 0.60$ in the absence of a control pulse (Figure 2).

In the presence of a control pulse with $\varepsilon_0 \neq 0$ in eq 14, the nondiagonal element $F_{01}$ couples the dressed ground state to the excited state, changing the topography of the potential energy surface. As shown in Figure 1, for a pulse with $\hbar\omega = 1.6$ eV the diabatic dressed state crosses the excited electronic potential at $\theta_{LIP} \approx 0.9$ rad, hence, the effect of the light-induced potential (shown in the inset of Figure 1) is most important in the neighborhood of $\theta_{LIP}$. Since the coupling between electronic states also depends on time via the pulse envelope function (eq 11), the effect on nonadiabatic dynamics also depends on the time delay of the control pulse relative to the initial vertical excitation. Figure 3 shows results of the trans $S_0$ population corresponding to different delay times of the control

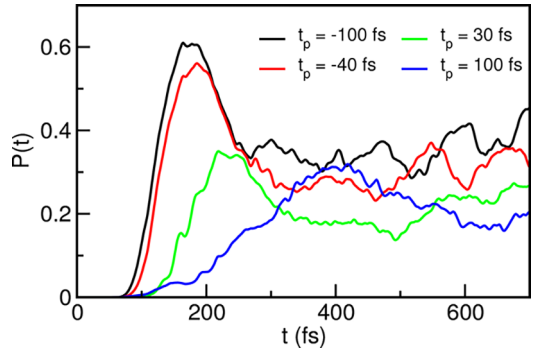


**Figure 3.** Time-dependent $S_0$ trans population dynamics in the presence of a 300 fs control field.



DOI: 10.1021/acs.jctc.7b01217
J. Chem. Theory Comput. 2018, 14, 1198−1205

pulse. At negative time delays, when the control pulse precedes the initial vertical excitation, the wave packet crosses the $\theta_{LIP}$ region before the coupling $F_{01}$ is active, and, hence, the dynamics of the trans population agrees with the dynamics of the system in the absence of the control pulse (Figure 2), so neither the isomerization time nor the efficiency are affected. However, as the pulse delay becomes positive, and the modulation of the PES via LIP precedes the wave packet propagation, the dynamics is strongly affected as shown by changes in the reaction time and efficiency. Note that for a pulse delay $t_p$ = 100 fs, the isomerization time $t_{MAX}$ > 400 fs—i.e., twice longer than without the control field.

To better quantify the effect of the LIP on the dynamics, Figure 4 shows $t_{MAX}$ and $P_{MAX}$ as a function of the control pulse

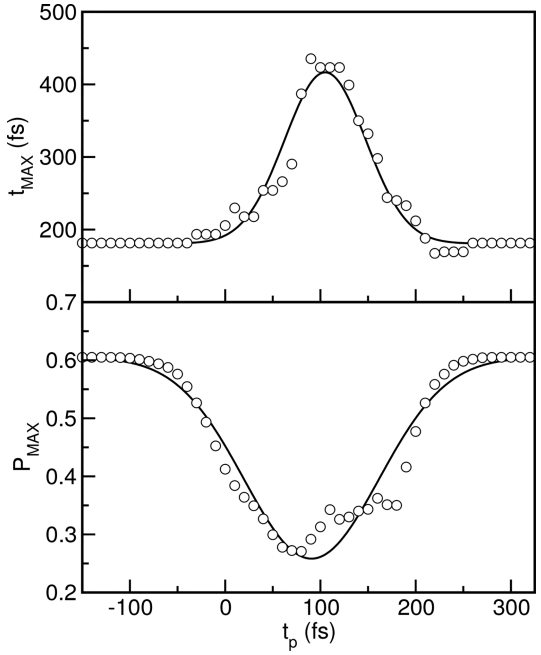


**Figure 4.** Dependence of $t_{MAX}$ (top) and $P_{MAX}$ (bottom) on the time delay ($t_p$) of a 300 fs control pulse. Solid lines are guides for the eyes.

time delay ($t_p$). The results show that there is an optimal pulse delay time that is able to delay the excited-state isomerization by more than 200 fs, although for such a control pulse the isomerization efficiency is reduced by about 50%. Therefore, the effect of the control pulse is predicted to be quite significant and clearly verified by femtosecond laser spectroscopy.

To rationalize and interpret our findings on quantum control, we applied Floquet theory which provides valuable insights on reaction channels and effective dressed potentials. In the dressed-state representation, the effect of the control field corresponds to a change of the potential energy surface—i.e., a light-induced potential energy change in the vicinity of $\theta_{LIP}$ (see the inset of Figure 1). The position of $\theta_{LIP}$ is governed by the frequency of the control field. Therefore, it is possible to tune the position of the crossing between the surfaces by changing $\omega$ and moving the LIP toward or away from the natural conical intersection. On the other hand, the coupling between the surfaces and hence the energy separation of the resulting avoiding crossing is controlled by the intensity profile of the pulse which defines the coupling $F_{01}$. Note that the resulting LIP is time-dependent as defined by the pulse envelope.

Figure 5 shows the evolution of the LIP as a function of time. As the field turns on, the coupling intensity increases, and the

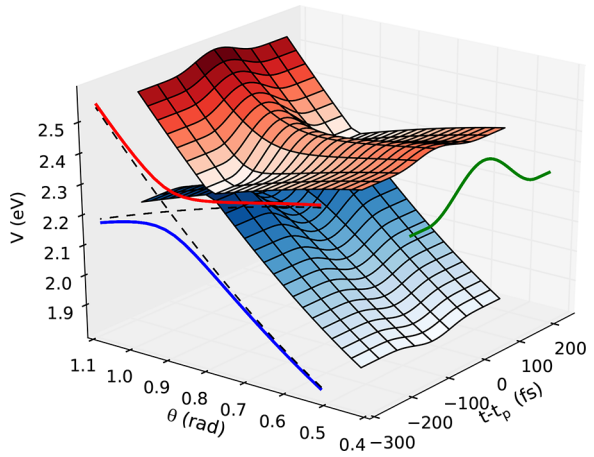


**Figure 5.** Time evolution of the LIP, along the dihedral angle for $x$ = 0, for a control field with $t_d$ = 300 fs. Color key: Red and blue solid curves show typical adiabatic light-induced potentials for the excited and dressed ground diabatic states (dashed lines). The red and blue surfaces show the time evolution of the upper and lower LIP, respectively. The energy separation between both surfaces depends on the envelope of the control pulse (shown as a green solid curve). For clarity, only the region near the LIP is shown.

energy difference between the two surfaces increases. After the separation between the two LIPs reaches a maximum value at $t = t_p$, the coupling diminishes, and the PES recovers the same shape as in the absence of any control field. Note that the excited LIP generated by the control field (red surface in Figure 5) exhibits a barrier at $\theta = \theta_{LIP}$, along the isomerization coordinate $\theta$. Therefore, the LIP is an effective "trap" that hinders the evolution of the wave packet toward the natural CI for as long as the control pulse is active.

To demonstrate the "trapping" effect of the LIP on the dynamics of isomerization, Figure 6 shows the evolution of the diabatic excited-state density reduced to the reaction coordinate $\theta$, as follows:

$$\rho(\theta; t) = \int dx \rho_{[1]}(\mathbf{x}; t) \tag{25}$$

The effect of a control pulse with $t_p$ = 100 fs (Figure 6, panel a) is compared to the corresponding dynamics in the absence of a control pulse (Figure 6, panel b). In the absence of the field, the wave packet initialized in the cis configuration ($|\theta| < \pi/2$ rad) evolves freely toward the trans configuration ($|\theta| > \pi/2$ rad), rapidly escaping from the cis region within about 100 fs. In the presence of the control field, the dynamics is quite different. Before the wavepacket reaches the surroundings of $\theta = \theta_{LIP}$ (marked with dotted lines in Figure 6), the dynamical evolution is the same as with no control pulse applied. However, as soon as the wavepacket enters the LIP region, it gets reflected in the excited-state surface and does not evolve toward the trans state. Note that since it takes about 80 fs for the initial wavepacket to reach the LIP, the control field is most effective when $t_p$ > 80 fs (as shown in Figure 4). However, while the pulse is interacting with the system, some population leaks into the lower LIP (colored blue in Figure 5), reducing the efficiency of the process. After the pulse is over, the wavepacket continues the evolution to the trans region,


DOI: 10.1021/acs.jctc.7b01217
J. Chem. Theory Comput. 2018, 14, 1198−1205

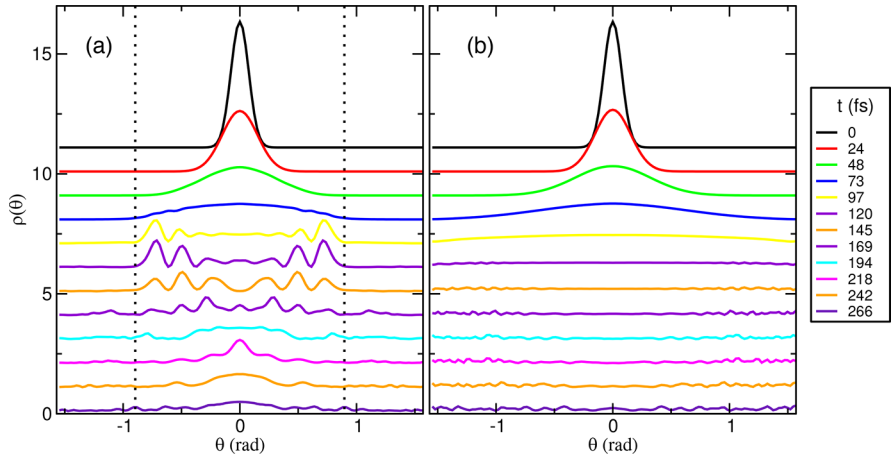


**Figure 6.** Time evolution of the reduced diabatic excited-state wave function (eq 25) for (a) a $t_p$ = 100 fs control field and (b) no control field applied. Dotted lines correspond to the position of $\theta_{LIP}$. For clarity, the wave functions are shifted vertically, and only the cis region is shown.

exhibiting a significant delay time for isomerization and reduced efficiency of cis/trans interconversion.

From our analysis, it is clear that the underlying quantum dynamics of isomerization depends on the characteristics of the LIP and, hence, on the parameters of the control pulse. In this sense, the intensity of the pulse ($\varepsilon_0$) controls the adiabatic separation of the LIP potentials and, hence, modulates the efficiency of the process as determined by branching processes and recombination into the cis conformation. In addition, $t_d$ defines the pulse width and determines the time period when the wave packet is influenced by the pulse. Thus, $t_d$ is a control parameter that can be used to manipulate (e.g., delay) the excited-state reaction dynamics. Therefore, it is clear that the pulse parameters can be chosen to achieve control over $t_{MAX}$ and $P_{MAX}$.

Figure 7 shows the effect of changes in the pulse time duration $t_d$ on $t_{MAX}$ and $P_{MAX}$, as a function of $t_p$. As expected from our earlier discussion, the shorter the pulse the less significant is the extent of control over $t_{MAX}$ and $P_{MAX}$.

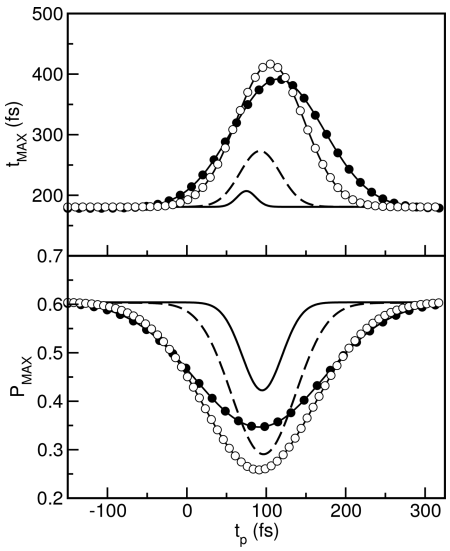


**Figure 7.** Dependence of $t_{MAX}$ (top) and $P_{MAX}$ (bottom) on the time delay ($t_p$) for different pulses profiles. Solid line: $\varepsilon_0$ = 0.01 au, $t_d$ = 50 fs. Dashed line: $\varepsilon_0$ = 0.01 au, $t_d$ = 150 fs. Open circles: $\varepsilon_0$ = 0.01 au, $t_d$ = 300 fs. Black circles: $\varepsilon_0$ = 0.02 au, $t_d$ = 300 fs.

Interestingly, while the isomerization time $t_{MAX}$ is quite sensitive to the pulse duration, the yield defined by $P_{MAX}$ can be quite comparable for pulses with different duration. For example, a pulse with $t_d$ = 150 fs gives an efficiency of isomerization comparable to the yield achievable with a pulse with $t_d$ = 300 fs. To modify the efficiency of the process, however, we can tune the intensity of the field. Figure 7 shows that for a pulse with $t_d$ = 300 fs, doubling the intensity parameter ($\varepsilon_0$) increases the yield from 25% to 35%. Note, however, that increasing the intensity of the field can initiate other processes such as multiphonon absorption, ionization, and formation of free radicals that are highly reactive and modify amino acid side chains.[56] None of these potential detrimental effects are included in the simple model Hamiltonian used in our study. Although the characterization of these processes would require the use of a more realistic model,[43−46] our results serve to gain valuable insights on the underlying control mechanism and suggest that it should be possible to control the cis−trans isomerization of rhodopsin by rational design of control pulses.

## 4. CONCLUDING REMARKS

We have shown that the dynamics of cis−trans isomerization of rhodopsin can be simulated and controlled by the influence of moderately strong femtosecond pulses, as described by explicit quantum dynamics simulations. We found that the time evolution of the wave packet in the adiabatic Floquet state representation based on an empirical 3-state 25-mode model Hamiltonian can be strongly influenced by a long (300 fs) control pulse when applied with a delay time $t_p$ > 80 fs, after photoexcitation of the system. We also found that it is possible to slow down the excited-state isomerization in a controllable way by simply changing the time delay of the control pulse. The underlying control mechanism is based on 'trapping' of the wave packet in the light-induced potential generated by the control field. Control for a wide range of pulses with different duration and intensity is demonstrated, showing that the duration of the control pulse is an important element in determining the amount of the control, whereas the intensity of the field controls the efficiency of the process. The reported results thus demonstrate the feasibility of manipulating the underlying ultrafast photoisomerization dynamics of a model visual pigment, as necessary for the development of ultrafast optical switches.



DOI: 10.1021/acs.jctc.7b01217
J. Chem. Theory Comput. 2018, 14, 1198−1205

Finally, we conclude from the results presented in Figures 4 and 7, and the analysis in terms of dressed states, that the simple control technique investigated in this paper is only able to slow down the isomerization, not to speed it up, or increase the efficiency. To increase the efficiency or speed up the reaction, sequences of pulses might be necessary as previously shown for control of tunneling dynamics[57−59] or control scheme based on pulse-shaping techniques[10] or incoherent control.[15]

## AUTHOR INFORMATION


### Corresponding Author

*E-mail: victor.batista@yale.edu.

### ORCID

Victor S. Batista: 0000-0002-3262-1237



### Funding

V.S.B. acknowledges support from the NSF Grant CHE-1465108 and high-performance computing time from National Energy Research Scientific Computing Center (NERSC) and the Yale High Performance Computing Center.


### Notes

The authors declare no competing financial interest.

## ACKNOWLEDGMENTS

The authors thank Erik T. J. Nibbering and Nimrod Moiseyev for stimulating discussions.

## REFERENCES


(1) Rice, S. A.; Zhao, M. *Optical Control of Molecular Dynamics*; Wiley-Interscience: New York, 2000; DOI: 10.1002/9783527639700.

(2) Shapiro, M.; Brumer, P. *Quantum Control of Molecular Processes*, 2nd ed. ed.; Wiley-Interscience: New York, 2012.

(3) Zewail, A. H. *Femtochemistry*; World Scientific: Singapore, 1994; Vol. *I and II*.

(4) Gamaly, E. *Femtosecond Laser-Matter Interaction: Theory, Experiments and Applications*; Pan Stanford Publishing Pte. Ltd.: Singapore, 2011.

(5) Judson, R. S.; Rabitz, H. Teaching lasers to control molecules. *Phys. Rev. Lett.* **1992**, *68*, 1500.

(6) Warren, W. S.; Rabitz, H.; Dahleh, M. Coherent control of quantum dynamics: the dream is alive. *Science* **1993**, *259*, 1581−1589.

(7) Krausz, F.; Ivanov, M. Attosecond physics. *Rev. Mod. Phys.* **2009**, *81*, 163.

(8) Sansone, G.; Benedetti, E.; Calegari, F.; Vozzi, C.; Avaldi, L.; Flammini, R.; Poletto, L.; Villoresi, P.; Altucci, C.; Velotta, R.; Stagira, S.; Silvestri, S. D.; Nisoli, M. Isolated Single-Cycle Attosecond Pulses. *Science* **2006**, *314*, 443.

(9) Goulielmakis, E.; Schultze, M.; Hofstetter, M.; Yakovlev, V. S.; Gagnon, J.; Uiberacker, M.; Aquila, A. L.; Gullikson, E. M.; Attwood, D. T.; Kienberger, R.; Krausz, F.; Kleineberg, U. Single-Cycle Nonlinear Optics. *Science* **2008**, *320*, 1614.

(10) Großmann, F.; Feng, L.; Schmidt, G.; Kunert, T.; Schmidt, R. Optimal control of a molecular cis-trans isomerization model. *EPL (Europhysics Letters)* **2002**, *60*, 201.

(11) Flores, S. C.; Batista, V. S. Model Study of Coherent-Control of the Femtosecond Primary Event of Vision. *J. Phys. Chem. B* **2004**, *108*, 6745−6749.

(12) Prokhorenko, V. I.; Nagy, A. M.; Waschuk, S. A.; Brown, L. S.; Birge, R. R.; Miller, R. D. Coherent control of retinal isomerization in bacteriorhodopsin. *Science* **2006**, *313*, 1257−1261.

(13) Chen, X.; Batista, V. S. The MP/SOFT methodology for simulations of quantum dynamics: Model study of the photo-isomerization of the retinyl chromophore in visual rhodopsin. *J. Photochem. Photobiol., A* **2007**, *190*, 274−282.

(14) Polli, D.; Altoe, P.; Weingart, O.; Spillane, K. M.; Manzoni, C.; Brida, D.; Tomasello, G.; Orlandi, G.; Kukura, P.; Mathies, R. A.; Garavelli, M.; Cerullo, G. Conical intersection dynamics of the primary photoisomerization event in vision. *Nature* **2010**, *467*, 440−443.

(15) Lucas, F.; Hornberger, K. Incoherent Control of the Retinal Isomerization in Rhodopsin. *Phys. Rev. Lett.* **2014**, *113*, 058301.

(16) Tscherbul, T. V.; Brumer, P. Quantum coherence effects in natural light-induced processes: cis-trans photoisomerization of model retinal under incoherent excitation. *Phys. Chem. Chem. Phys.* **2015**, *17*, 30904−30913.

(17) Birge, R. R.; Gillespie, N. B.; Izaguirre, E. W.; Kusnetzow, A.; Lawrence, A. F.; Singh, D.; Song, Q. W.; Schmidt, E.; Stuart, J. A.; Seetharaman, S.; Wise, K. J. Biomolecular Electronics: Protein-Based Associative Processors and Volumetric Memories. *J. Phys. Chem. B* **1999**, *103*, 10746−10766.

(18) Floquet, G. Sur les equations differentielles lineaires a coefficients periodiques. *Ann. Sci. École Norm. Sup.* **1883**, *12*, 47.

(19) Shirley, J. H. Solution of the Schrödinger Equation with a Hamiltonian Periodic in Time. *Phys. Rev.* **1965**, *138*, B979−B987.

(20) Chu, S. Floquet theory and complex quasivibrational energy formalism for intense field molecular photodissociation. *J. Chem. Phys.* **1981**, *75*, 2215−2221.

(21) Chu, S.-I.; Telnov, D. A. Beyond the Floquet theorem: generalized Floquet formalisms and quasienergy methods for atomic and molecular multiphoton processes in intense laser fields. *Phys. Rep.* **2004**, *390*, 1−131.

(22) Halasz, G. J.; Vibok, A.; Sindelka, M.; Cederbaum, L. S.; Moiseyev, N. The effect of light-induced conical intersections on the alignment of diatomic molecules. *Chem. Phys.* **2012**, *399*, 146−150.

(23) Pawlak, M.; Moiseyev, N. Light-induced conical intersection effect enhancing the localization of molecules in optical lattices. *Phys. Rev. A: At., Mol., Opt. Phys.* **2015**, *92*, 023403.

(24) Moiseyev, N.; Milan, S.; Lorenz, S. C. Laser-induced conical intersections in molecular optical lattices. *J. Phys. B: At., Mol. Opt. Phys.* **2008**, *41*, 221001.

(25) Chang, B. Y.; Rabitz, H.; Sola, I. R. Light-induced trapping of molecular wave packets in the continuum. *Phys. Rev. A: At., Mol., Opt. Phys.* **2003**, *68*, 031402.

(26) Chang, B. Y.; Lee, S.; Sola, I. R. Stationary molecular wave packets at nonequilibrium nuclear configurations. *J. Chem. Phys.* **2004**, *121*, 11118.

(27) Chang, B. Y.; Sola, I. R.; Shin, S. Molecular events in the light of strong fields: A light-induced potential scenario. *Int. J. Quantum Chem.* **2016**, *116*, 608−621.

(28) Halász, G. H.; Agnes, V.; Milan, S.; Nimrod, M.; Lorenz, S. C. Conical intersections induced by light: Berry phase and wavepacket dynamics. *J. Phys. B: At., Mol. Opt. Phys.* **2011**, *44*, 175102.

(29) Šindelka, M.; Nimrod, M.; Lorenz, S. C. Strong impact of light-induced conical intersections on the spectrum of diatomic molecules. *J. Phys. B: At., Mol. Opt. Phys.* **2011**, *44*, 045603.

(30) Halász, G. J.; Agnes, V.; Nimrod, M.; Lorenz, S. C. Light-induced conical intersections for short and long laser pulses: Floquet and rotating wave approximations versus numerical exact results. *J. Phys. B: At., Mol. Opt. Phys.* **2012**, *45*, 135101.

(31) Halasz, G. J.; Sindelka, M.; Moiseyev, N.; Cederbaum, L. S.; Vibok, A. Light-Induced Conical Intersections: Topological Phase, Wave Packet Dynamics, and Molecular Alignment. *J. Phys. Chem. A* **2012**, *116*, 2636−2643.

(32) Halasz, G. J.; Vibok, A.; Meyer, H.-D.; Cederbaum, L. S. Effect of Light-Induced Conical Intersection on the Photodissociation Dynamics of the D2+ Molecule. *J. Phys. Chem. A* **2013**, *117*, 8528−8535.

(33) Halász, G. J.; Vibok, A.; Moiseyev, N.; Cederbaum, L. S. Nuclear-wave-packet quantum interference in the intense laser dissociation of the $D_2^+$ molecule. *Phys. Rev. A: At., Mol., Opt. Phys.* **2013**, *88*, 043413.

(34) Moiseyev, N.; Milan, S. The effect of polarization on the light-induced conical intersection phenomenon. *J. Phys. B: At., Mol. Opt. Phys.* **2011**, *44*, 111002.

(35) Cederbaum, L. S.; Chiang, Y.-C.; Demekhin, P. V.; Moiseyev, N. Resonant Auger Decay of Molecules in Intense X-Ray Laser Fields: Light-Induced Strong Nonadiabatic Effects. *Phys. Rev. Lett.* **2011**, *106*, 123001.
(36) Demekhin, P. V.; Cederbaum, L. S. Light-induced conical intersections in polyatomic molecules: General theory, strategies of exploitation, and application. *J. Chem. Phys.* **2013**, *139*, 154314.
(37) Corrales, M. E.; Gonzalez-Vazquez, J.; Balerdi, G.; Sola, I. R.; de Nalda, R.; Banares, L. Control of ultrafast molecular photodissociation by laser-field-induced potentials. *Nat. Chem.* **2014**, *6*, 785−790.
(38) Kim, J.; Hongli, T.; Todd, J. M.; Phil, B. Ab initio multiple spawning on laser-dressed states: a study of 1,3-cyclohexadiene photoisomerization via light-induced conical intersections. *J. Phys. B: At., Mol. Opt. Phys.* **2015**, *48*, 164003.
(39) Hahn, S.; Stock, G. Femtosecond secondary emission arising from the nonadiabatic photoisomerization in rhodopsin. *Chem. Phys.* **2000**, *259*, 297−312.
(40) Hahn, S.; Stock, G. Quantum-Mechanical Modeling of the Femtosecond Isomerization in Rhodopsin. *J. Phys. Chem. B* **2000**, *104*, 1146−1149.
(41) Lin, S. W.; Groesbeek, M.; van der Hoef, I.; Verdegem, P.; Lugtenburg, J.; Mathies, R. A. Vibrational assignment of torsional normal modes of rhodopsin: Probing excited-state isomerization dynamics along the reactive C11 C12 torsion coordinate. *J. Phys. Chem. B* **1998**, *102*, 2787−2806.
(42) Wang, Q.; Schoenlein, R. W.; Peteanu, L. A.; Mathies, R. A.; Shank, C. V. Vibrationally coherent photochemistry in the femtosecond primary event of vision. *Science* **1994**, *266*, 422−422.
(43) Gascón, J. A.; Batista, V. S. QM/MM Study of Energy Storage and Molecular Rearrangements Due to the Primary Event in Vision. *Biophys. J.* **2004**, *87*, 2931−2941.
(44) Gascón, J. A.; Sproviero, E. M.; Batista, V. S. QM/MM Study of the NMR Spectroscopy of the Retinyl Chromophore in Visual Rhodopsin. *J. Chem. Theory Comput.* **2005**, *1*, 674−685.
(45) Gascón, J. A.; Sproviero, E. M.; Batista, V. S. Computational Studies of the Primary Phototransduction Event in Visual Rhodopsin. *Acc. Chem. Res.* **2006**, *39*, 184−193.
(46) Guo, Y.; Hendrickson, H. P.; Videla, P. E.; Chen, Y.-N.; Ho, J.; Sekharan, S.; Batista, V. S.; Tully, J. C.; Yan, E. C. Y. Probing the remarkable thermal kinetics of visual rhodopsin with E181Q and S186A mutants. *J. Chem. Phys.* **2017**, *146*, 215104.
(47) Peskin, U.; Moiseyev, N. The solution of the time-dependent Schrodinger equation by the (t,t') method: Theory, computational algorithm and applications. *J. Chem. Phys.* **1993**, *99*, 4590.
(48) Hanasaki, K.; Takatsuka, K. Unified treatment of field-induced and intrinsic nonadiabatic transitions with a generalized Floquet Hamiltonian method. *Phys. Rev. A: At., Mol., Opt. Phys.* **2013**, *88*, 053426.
(49) Feit, M. D.; Fleck, J. A. Solution of the Schrödinger equation by a spectral method II: Vibrational energy levels of triatomic molecules. *J. Chem. Phys.* **1983**, *78*, 301−308.
(50) Feit, M. D.; Fleck, J. A.; Steiger, A. Solution of the Schrödinger equation by a spectral method. *J. Comput. Phys.* **1982**, *47*, 412−433.
(51) Kosloff, D.; Kosloff, R. A fourier method solution for the time dependent Schrödinger equation as a tool in molecular dynamics. *J. Comput. Phys.* **1983**, *52*, 35−53.
(52) Gerber, R.; Buch, V.; Ratner, M. A. Time-dependent self-consistent field approximation for intramolecular energy transfer. I. Formulation and application to dissociation of van der Waals molecules. *J. Chem. Phys.* **1982**, *77*, 3022−3030.
(53) Swope, W. C.; Andersen, H. C.; Berens, P. H.; Wilson, K. R. A computer simulation method for the calculation of equilibrium constants for the formation of physical clusters of molecules: Application to small water clusters. *J. Chem. Phys.* **1982**, *76*, 637−649.
(54) Balzer, B.; Hahn, S.; Stock, G. Mechanism of a photochemical funnel: a dissipative wave-packet dynamics study. *Chem. Phys. Lett.* **2003**, *379*, 351−358.
(55) Balzer, B.; Stock, G. Modeling of decoherence and dissipation in nonadiabatic photoreactions by an effective-scaling nonsecular Redfield algorithm. *Chem. Phys.* **2005**, *310*, 33−41.
(56) Wang, J.; Askerka, M.; Brudvig, G.; Batista, V. Insights into Photosystem II from Isomorphous Difference Fourier Maps of Femtosecond X-ray Diffraction Data and Quantum Mechanics/Molecular Mechanics Structural Models. *ACS Energy Lett.* **2017**, *2*, 397−407.
(57) Rego, L. G. C.; Abuabara, S. G.; Batista, V. S. Coherent Optical Control of Electronic Excitations in Functionalized Semiconductor Nanostructures. *Quantum Information and Computation* **2005**, *5*, 318−334.
(58) Rego, L. G.; Santos, L. F.; Batista, V. S. Coherent Control of Quantum Dynamics with Sequences of Unitary Phase-Kick Pulses. *Annu. Rev. Phys. Chem.* **2009**, *60*, 293−320.
(59) Saha, R.; Markmann, A.; Batista, V. S. Tunneling through Coulombic barriers: quantum control of nuclear fusion. *Mol. Phys.* **2012**, *110*, 995−999.


DOI: 10.1021/acs.jctc.7b01217
*J. Chem. Theory Comput.* 2018, 14, 1198−1205